Bioconjugate Chemistry

Article

pubs.acs.org/bc

Site-Specific PEGylation of HR2 Peptides: Effects of PEG Conjugation Position and Chain Length on HIV-1 Membrane Fusion Inhibition and Proteolytic Degradation

Maarten Danial,[‡] Tim H. H. van Dulmen,[‡] Joanna Aleksandrowicz,[†] Andy J. G. Pötgens,[†] and Harm-Anton Klok*,[‡]

[‡]École Polytechnique Fédérale de Lausanne, Institut des Matériaux and Institut des Sciences et Ingénierie Chimiques, Laboratoire des Polymères, Bâtiment MXD, 1015 Lausanne, Switzerland

[†]AplaGen GmbH, Arnold Sommerfeld-Ring 2, D-52499, Baesweiler, Germany

Supporting Information

ABSTRACT: Peptides derived from the HR1 or HR2 regions of the HIV-1 envelope glycoprotein gp41 have been shown to be effective inhibitors to prevent virus−host cell membrane fusion. These peptide drugs, however, suffer from relatively short plasma half-lives and are susceptible to enzymatic degradation. Modification of peptides/proteins with poly(ethylene glycol) (PEG) is a well-established strategy to overcome these limitations. This manuscript presents the results of a systematic study on the influence of the site of PEGylation of HR2-derived peptides, as well as of PEG molecular weight on the biological activity and proteolytic stability of these conjugates. Investigation of the fusion inhibitory efficacy of the conjugates in a model cell−cell based assay revealed a loss in activity for the PEGylated peptides as compared to the wild-type HR2-derived peptide. The loss of activity, however, can be minimized by controlling the site of PEGylation, more specifically, by introducing the PEG chain at one of the more central positions along the non-interacting α-helical surface of the peptides. The proteolytic stability of the PEG−peptide conjugates was assessed in a trypsin-based model assay, which revealed an up to 3.4-fold increase in degradation half-life that may help to compensate for the lower inhibitory efficacy of the PEG−peptide conjugates as compared to the wild-type peptide. The results of this study emphasize the power of site-specific PEGylation to improve the stability of peptide/protein drugs while minimizing adverse effects on biological activity.

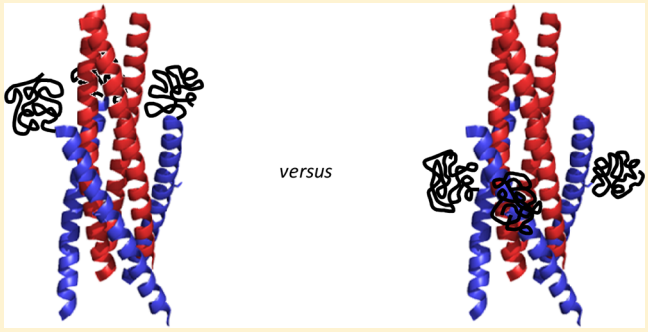

INTRODUCTION

It has been estimated that 33 million people worldwide have been infected by the human immunodeficiency virus type 1 (HIV-1).[1] Despite being a pandemic, there is no cure against this virus that can lead to acquired immune deficiency syndrome (AIDS). Nevertheless, a number of drug therapies are available nowadays that can delay the onset of AIDS, which include entry/fusion inhibitors, reverse transcriptase inhibitors, protease inhibitors, and integrase inhibitors.[2] From these therapies, fusion and entry inhibitors are a particularly intriguing therapeutic option since these prohibit the virus from entering the cell. Moreover, the application of effective fusion/entry inhibitors may reduce the need for the conventional reverse transcriptase, integrase, and protease inhibitors. One such fusion inhibitor, T-20 (Fuzeon, Enfuvirtide), which was approved in 2003, is a peptide drug derived from the gp41 HR2 domain that competitively inhibits the fusion process between the viral and host cell membranes.[3−5]

While T-20 has been shown to be very effective in preventing virus−host cell membrane fusion and reducing viral loads in HIV-1-infected individuals,[6] it also suffers from the same drawbacks as other protein/peptide drugs, i.e., short plasma half-lives (∼3.8 h)[6] and susceptibility to proteolytic degradation. This is nicely illustrated by the fact that treatment with T-20 requires two daily subcutaneous injections of 90 mg each in order to maintain an effective therapeutic concentration.[6] A widely used and effective strategy to increase the plasma half-life of protein/peptide drugs and prevent proteolytic degradation involves their modification with poly(ethylene glycol) (PEG).[7−11] Mono-PEGylation of interferon α-2a with a 40 kDa branched PEG derivative, for example, has been shown to result in a 70-fold increase in serum half-life and a 50-fold increase in mean plasma residence time.[12] Interestingly, the *in vitro* activity of the PEGylated protein was only 7% of that of the unmodified analogue, while a several-fold increase in *in vivo* activity was observed upon PEGylation.[12] In another example, site-specific PEGylation of erythropoiesis protein was found to

Received: April 22, 2012
Revised: June 22, 2012
Published: July 9, 2012

lead to a 2-fold increase in elimination half-life and mean residence time, while maintaining cell proliferation activity.[13]

Whereas early PEGylation strategies only provided little or no control over the degree and site of conjugation, a variety of approaches is available nowadays that allow access to well-defined PEG−peptide/protein conjugates where these parameters can be accurately controlled.[14,15] The ability to site-specifically modify peptides and proteins is of critical importance to generate biologically active PEG−peptide/protein conjugates.[16] Doherty et al., for example, prepared and PEGylated a library of 13 cysteine analogues of the granulocyte macrophage colony-stimulating factor (GM-CSF).[17] By targeting regions of the protein that are located away from the active sites, a variety of PEGylated GM-CSF analogues was obtained that possessed biological activities comparable to that of the wild-type protein. In another study, Salhanick et al. compared the biological activity of N- and C-terminal PEGylated glucose-dependent insulinotropic polypeptide (GIP).[18] Whereas N-terminal PEGylation essentially resulted in a complete loss of activity, C-terminal modification only modestly affected functional activity. Yamamoto et al. prepared and investigated the biological activity of a site-specifically mono-PEGylated variant of tumor necrosis factor-α (TNF-α).[19] Site-specific PEGylation was found to result in PEG−protein conjugates that possessed 80% of the activity of the unmodified wild-type TNF-α, whereas random PEGylation resulted in conjugates that only showed 10% residual activity.

One possible strategy to improve the pharmacokinetics and *in vivo* half-life of peptide-based HIV-1 fusion inhibitors involves the design of variants ("third-generation fusion inhibitors") that contain stabilizing intramolecular salt bridges or covalent bonds.[5] A second option is the use of protease-resistant D-peptide based inhibitors.[20] Site-specific polymer (or more specifically, poly(ethylene glycol) (PEG) modification) is a third possibility. Whereas site-specific polymer/PEG modification of proteins and peptides is well-established (*vide supra*), this strategy has only been explored to a limited extent to improve the stability and half-life of peptide-based HIV-1 fusion inhibitors. In a patent application, Bailon and Won describe the preparation and antiviral activity of two N-terminal PEGylated T20 variants, which were found to possess IC_{50} values that are approximately one order of magnitude higher as compared to the unmodified T20 peptide.[21] In a second patent, Bailon and Won describe the PEGylation at the N-terminus of a T20 peptide variant known as T1249.[22] The T1249−PEG20k conjugate was found to have 13.7−56.7-fold reduction in anti-HIV activity (IC_{50} = 0.041 to 0.170 μg/mL) relative to the unmodified T1249 peptide (IC_{50} = 0.003 μg/mL). Others have explored the conjugation of peptide-based HIV-1 fusion inhibitors to biological macromolecules in order to develop long-lasting conjugates.[23,24] Stoddart et al. studied the *in vitro* anti-HIV activity of human serum albumin conjugates of the C34 peptide fusion inhibitor, where the human serum albumin was covalently attached via a maleimide linker to the N- or C-terminus of the peptide.[23] The N-terminal human serum albumin conjugates showed only minor losses in anti-HIV activity ($IC_{50} \approx 2$ nM) relative to the C34 peptide (IC_{50} = 0.6 nM). Conversely, C-terminal human serum albumin−C34 conjugates showed an order of magnitude loss in antiviral activity (IC_{50} = 11.2 nM). The human serum albumin conjugated to the N-terminus of C34 was shown to take more than 96 h for complete renal elimination compared to ~10 h for the C34 peptide alone. In another example, Huet et al. reported the development of long-lasting T-20 variants, which were obtained by N-terminal modification of the peptide with an anti-thrombin-binding carrier pentasaccharide.[24] These saccharide−peptide conjugates were found to possess an elimination half-life of more than 10 h in rat plasma as compared to 2.8 h for the unmodified peptide. In the examples discussed above, however, no efforts were reported to systematically study and understand the effects of the site of polymer conjugation on the biological activity and stability of the fusion inhibitors. This manuscript describes the preparation of a library of PEGylated HR2 derivatives and systematically studies the influence of the site of PEGylation and PEG molecular weight on the biological activity and proteolytic stability of the conjugates. The fusion inhibitory efficacy of the polymer conjugates was studied using a model syncytia assay, whereas the proteolytic stability of the PEG−peptide conjugates was assessed in a trypsin-based model assay.

EXPERIMENTAL SECTION

Materials. Rink amide AM resin (mesh 200−400 with 0.61 mmol·g^{-1} loading), Fmoc-L-Ala-OH, Fmoc-L-Arg(Pbf)−OH, Fmoc-L-Asn(Trt)−OH, Fmoc-L-Asp(OtBu)−OH, Fmoc-L-Cys(Trt)−OH, Fmoc-L-Gln(Trt)−OH, Fmoc-L-Glu(OtBu)−OH, Fmoc-Gly-OH, Fmoc-L-His(Trt)−OH, Fmoc-L-Ile-OH, Fmoc-L-Leu-OH, Fmoc-L-Lys(Boc)−OH, Fmoc-L-Phe-OH, Fmoc-L-Ser(tBu)−OH, Fmoc-L-Thr(tBu)−OH, Fmoc-L-Trp(Boc)−OH, Fmoc-L-Tyr(tBu)−OH, and Fmoc-L-Val-OH, as well as hydroxybenzotriazole (HOBT) and 2-(6-chloro-1*H*-benzotriazole-1-yl)-1,1,3,3-tetramethylaminium hexafluorophosphate (HCTU), were all purchased from IRIS Biotech (Marktredwitz, Germany). Piperidine (99%), diisopropylethylamine (DIPEA, 99%), trypsin DPCC treated type XI from bovine pancreas, phenylmethanesulfonyl fluoride (PMSF), triethylamine (Et_3N, >99%), acryloyl chloride (97%), and phosphate buffered saline (PBS) sachets were purchased from Sigma-Aldrich (Buchs, Switzerland). Celltracker Green (CTgreen) and Celltracker Orange (CTorange) were obtained from Invitrogen, dissolved at 5 mM in DMSO and stored in aliquots at −20 °C in the dark. Dulbecco's PBS (containing 10 mM of sodium phosphate) and Hank's balanced salt solution (HBSS) were purchased from Invitrogen (Karlsruhe, Germany). *N*,*N*-dimethylformamide (DMF) and acetonitrile (HPLC grade) were obtained from VWR (Nyon, Switzerland). *N*-Methylpyrrolidone (NMP) and diethyl ether (Et_2O) were obtained from Schweizerhall (Basel, Switzerland).

Cell Lines. Chinese hamster ovarian (CHO-WT) cells that express the wild-type HIV-1 envelope glycoprotein gp120 were obtained through the AIDS Research and Reference Reagent Program, Division of AIDS, NIAID, NIH from Judith M. White.[25] To preserve the expression of the HIV-1 gp120 protein, CHO-WT cells were maintained in glutamine-deficient GMEM medium (a modification of MEM-alpha medium, PAN Biotech, Aidenbach, Germany) to which L-glutamic acid (final conc. 0.2942 g·L^{-1}), L-asparagine (final conc. 0.03020 g·L^{-1}), Na-pyruvate (final conc. 0.22 g·L^{-1}), and non-essential amino acids L-alanine (0.01782 g·L^{-1}), L-aspartic acid (final conc. 0.2662 g·L^{-1}), glycine (final conc. 0.01501 g·L^{-1}), L-proline (final conc. 0.06906 g·L^{-1}), and L-serine (0.02102 g·L^{-1}) (all from Sigma Aldrich, Taufkirchen, Germany) were added, together with 400 μM methionine sulfoximine (Sigma Aldrich, Schnelldorf, Germany), 1% penicillin/streptomycin, 1% amphotericin B, and 10% fetal calf serum (FCS, Sigma Aldrich). Adherent CHO-WT cells were passaged using

dx.doi.org/10.1021/bc3002248 | *Bioconjugate Chem.* 2012, 23, 1648−1660

trypsin/ethylene diamine tetraacetic acid (EDTA). SupT1 cells (containing the CD4 HIV receptor) and K562 cells (lacking CD4) were obtained from DSMZ (Braunschweig, Germany) and grown in suspension in Roswell Park Memorial Institute (RPMI) medium (Invitrogen, Karlsruhe, Germany) with 1% penicillin/streptomycin, 1% amphotericin B, and 10% FCS, as recommended by the supplier. All cell lines were passaged for a maximum of four weeks, at which point a new batch of cells was thawed and cultured.

Peptide Synthesis and Purification. All peptides were synthesized using a CEM Liberty automated microwave peptide synthesizer on a 0.25 mmol scale by Fmoc chemistry on a Rink amide AM resin (0.61 mmol·g^{-1} loading). Fmoc deprotection was achieved in two subsequent steps using 20% piperidine with 0.1 M HOBT in DMF (to reduce racemization[26]) for 1 min and subsequently 6 min using 56 W of microwave power at 75 ± 5 °C. After that, the resin was washed with five 10 mL portions of DMF and cooled to approximately 25 °C. A single 0.2 M (1 mmol, 5 mL) amino acid coupling for each residue of the sequence was performed with stock solutions of 0.5 M HOBT/HCTU in DMF (1 mmol, 2 mL) as the activator mixture and 2 M DIPEA in NMP (2 mmol, 1 mL) as the base. The final molar ratio with respect to the Rink amide AM resin for amino acid/activator/base during the reaction was 4:4:8 and the coupling reaction proceeded for 7 min using 24 W of microwave power at 60 ± 5 °C per the manufacturer's protocol.[26] After completion of the synthesis, the peptide was cleaved from the resin and deprotected using 10 mL of a mixture of trifluoroacetic acid (TFA), triisopropylsilane (TIS), and Milli-Q water (~18 MΩ cm, Millipore) in the volume ratio 95:2.5:2.5% for 3.5−4 h at room temperature.

All peptides were purified by preparative high-pressure liquid chromatography (HPLC) using a Waters 600 automated gradient controller pump module connected to a Waters prep degasser system. Sample elution was monitored by a Waters 2487 dual λ absorbance detector and peptides collected using a Waters fraction collector III. Purification was achieved with an Atlantis OBD C-18 reverse-phase column (5 μm, 30 × 150 mm, Waters) using water/TFA (0.1% TFA in water, Solvent A) and acetonitrile/TFA (0.1% TFA in acetonitrile, Solvent B) as the mobile phase. Elution was achieved at 20 mL/min by typically running gradients of 40−50% solvent B over 20 min. All peptides were purified to at least 95% by preparative HPLC and verified for purity by analytical HPLC using a monomeric C-18 column (5 μm, 4.6 × 150 mm, 238TP5415, Vydac). Fractions containing peptide were detected by UV absorbance at 220 and 280 nm. The molecular masses of the peptides were confirmed by electrospray ionization mass spectrometry (ESI-MS) or MALDI-TOF using α-cyano-4-hydroxycinnamic acid as the matrix as described below. All peptide samples were freeze−dried yielding a white powder.

Synthesis of Monomethoxy-PEG-Acrylates. Monomethoxy-PEG750-OH (mPEG−OH, 5.0 g, 6.7 mmol) was dried azeotropically in 50 mL dry toluene through rotary evaporation. After that, the resulting mPEG−OH melt was placed on ice and dissolved in 300 mL dry dichloromethane (DCM). After addition of Et_3N (1.86 mL, 2.0 equiv), acryloyl chloride (0.81 mL, 1.5 equiv) was added dropwise over a period of 30 min. The reaction was allowed to proceed with stirring overnight in the dark at room temperature under nitrogen. After that, the resulting pale yellow solution was extracted twice with 5% HCl, twice against 5% NaOH, once against saturated $NaHCO_3$, and once against brine. The DCM layer was collected and dried over $MgSO_4$, and the volume of the solution was reduced to approximately 5 mL using rotary evaporation. After addition of 80 mL of Et_2O and storage at −20 °C overnight, the desired mPEG was precipitated, isolated by filtration, and dried *in vacuo*. Yield: 42%; conversion OH to acrylate: 95% (from ^{1}H NMR analysis). ^{1}H NMR ($CDCl_3$, 400 MHz): 6.4 ppm (dd, 1H, C***H***$_2$CHOOCH$_2$CH$_2$−PEG chain), 6.1 (dd, 1H, CH$_2$C***H***OOCH$_2$CH$_2$−PEG chain), 5.8 ppm (dd, 1H, C***H***$_2$CHOOCH$_2$CH$_2$−PEG chain), 4.3 ppm (t, 2H, CH$_2$CHOOC***H***$_2$CH$_2$−PEG chain), 3.6 ppm (m, 68H, PEG chain protons), 3.3 ppm (s, 3H, methoxy).

The protocol outlined above was also used to prepare mPEG2000-acrylate from mPEG2000-OH. Yield: 77%; conversion OH to acrylate: 95% (from ^{1}H NMR analysis). ^{1}H NMR ($CDCl_3$, 400 MHz): 6.4 ppm (dd, 1H, C***H***$_2$CHOOCH$_2$CH$_2$−PEG chain), 5.8 ppm (dd, 1H, C***H***$_2$CHOOCH$_2$CH$_2$−PEG chain), 6.1 ppm (dd, 1H, CH$_2$C***H***OOCH$_2$CH$_2$−PEG chain), 4.3 ppm (t, 2H, CH$_2$CHOOC***H***$_2$CH$_2$−PEG chain), 3.6 ppm (m, 180H, PEG chain protons), 3.3 ppm (s, 3H, methoxy). ^{1}H NMR and MALDI-ToF mass spectra of mPEG750-acrylate and mPEG2000-acrylate are included in the Supporting Information (Figure S1 and Figure S2).

Peptide PEGylation. PEGylation was typically carried out with 1.60 μmol (approximately 8 mg) of peptide dissolved in 4 mL of a 10 mM sodium phosphate buffer (pH 7.4). Then, 40 μmol (25 equiv) of the dry mPEG-acrylate was added to the reaction mixture. The peptide-PEG750 and peptide-PEG2000 reaction mixtures were allowed to stir at room temperature in the dark for approximately 44−48 h. After that, the peptide-mPEG conjugates were purified with preparative RP-HPLC using a 20 min solvent gradient from 40/60% acetonitrile/water (with 0.1% TFA) to 50/50% acetonitrile/water (with 0.1% TFA). The conjugate fractions were freeze−dried and lyophilized to yield a white powder (yield: 60−90%). MALDI-ToF mass spectra of all synthesized conjugates are included in the Supporting Information (Figure S3 and Figure S4).

Matrix Assisted Laser Desorption Ionization−Time of Flight Mass Spectrometry (MALDI-ToF MS). MALDI-ToF MS was carried out on a Shimadzu Axima-CFR plus MALDI-ToF mass spectrometer operating in the linear mode in the 500−14 000 m/z range. For the characterization of the mPEG-OH and mPEG-acrylates, saturated dithranol matrix in dichloromethane (DCM) with 30 wt % sodium trifluoroacetate (Na TFA) was used. This was mixed in a 1:1 volume ratio with the mPEG-OH or mPEG-acrylate (1 mg·mL^{-1}) dissolved in DCM from which 1 μL was applied onto the plate. For analysis of the peptides and the mPEG-peptide conjugates, a 10 mg·mL^{-1} THF solution of α-cyano-4-hydroxycinnamic acid was used to prepare the matrix. The matrix solution was mixed in a 1:1 volume ratio with the mPEG-peptide conjugates dissolved in Milli-Q water (1 mg·mL^{-1}). The samples were placed on the MALDI-ToF plate and allowed to dry. Calibration was achieved using several references: Angiotensin II ([M+H$^+$] = 1045.54), adrenocorticotropic hormone$_{18-39}$ (ACTH$_{18-39}$) peptide fragment ([M+H$^+$] = 2464.20), and bovine insulin ([M+H$^+$] = 5729.61). Measurements were performed with a laser power of 45−65 (max. laser power: 180).

Circular Dichroism Spectroscopy. Circular dichroism (CD) spectroscopy measurements were performed on a JASCO-715 spectropolarimeter equipped with a water bath and a PTC-348WI Peltier temperature controller. All samples were dissolved at approximately 1 mg·mL^{-1} in 10 mM

phosphate buffered saline (PBS, pH 7.4) and then diluted to a working concentration of 20 μM. The concentration of the peptides was verified by UV−vis spectroscopy using the extinction coefficient of the peptides at 280 nm determined using the linear combination of extinction coefficients of tyrosine (1490 $M^{-1}\cdot cm^{-1}$) and tryptophan (5500 $M^{-1}\cdot cm^{-1}$).[27] Experiments were carried out in a 0.1 cm path length quartz cuvette in the range 260−200 nm. All CD spectra were corrected for the baseline of 10 mM PBS (pH 7.4) and converted to mean residue ellipticity (MRE). α-Helix contents were calculated as follows:

$$\alpha\text{-helix content} = [\theta]_{222}/[\theta]_{222}^{100\%} \quad (1)$$

where $[\theta]_{222}^{100\%}$ is the theoretical mean residue ellipticity of a peptide with n residues with 100% α-helix content as defined by[28]

$$[\theta]_{222}^{100\%} = -40000\cdot(1 - 4.6/n) \quad (2)$$

Analytical Ultracentrifugation. Sedimentation equilibrium experiments were performed on a Beckman Optima XL-I analytical ultracentrifuge (Beckman, Palo Alto, CA, USA) at 20 °C. Six-channel quartz cells were used with an An-60 titanium rotor. All samples were dissolved in 10 mM PBS, pH 7.4, to a working concentration of 20 μM (or 10 μM PEG conjugate with 10 μM N45). Samples were initially scanned at 5000 rpm to identify appropriate wavelengths for data collection. The cells were scanned using a step size of 0.001 cm, and the data points were averaged over 6 replicates. The samples were then scanned at 280 nm at 20 000 or 25 000 rpm until two equilibrium curves taken 6 h apart were perfectly superimposed. The solvent density (ρ = 1.00534 $g\cdot mL^{-1}$) and partial specific volume of the peptide was calculated using the program *SEDNTERP* ($\bar{\nu}$ = 0.7293 $mL\cdot g^{-1}$ for the WT peptide).[29] The partial specific volumes of the S15C-PEG750 and S15C-PEG2000 conjugates were calculated to be 0.7435 and 0.7584 $mL\cdot g^{-1}$, respectively, by a weighted average of specific volumes between the peptide and PEG (0.833 $mL\cdot g^{-1}$). The sedimentation equilibrium data were then fitted to several models to reflect the oligomeric state of the system using the *Sedphat* program[30] as has been described with similar peptides.[31] The data were fitted with a "single species of interacting system" model, which yields a molecular weight of the sample. For all samples, the molecular weights of the samples were deemed reliable when the residuals between the fit and the data points was random around zero.

Trypsin Degradation Assay. Solutions of bovine trypsin (2 μM) and the peptide or PEG−peptide conjugate (20 μM) in 10 mM PBS (pH 7.4) were freshly prepared at room temperature. The concentrations of the solutions were verified by UV−vis spectroscopy as described in the section on CD spectroscopy (*vide supra*). A 1 mL aliquot of trypsin solution was warmed to 37 °C for exactly 5 min, and 1 mL of peptide or PEG−peptide conjugation solution was subsequently added. To stop the degradation, 50 μL samples were taken from the reaction mixture and added to 50 μL of a freshly prepared solution containing 5% acetic acid with 5 mM PMSF. Peptide degradation was monitored by analytical reverse-phase HPLC using a C-18 monomeric column (S/N E950404−10−3, Vydac) and a gradient of 5−95% acetonitrile (with 0.1% TFA) against water (with 0.1% TFA) over 16 min for sample elution. Sample elution was monitored using a UV−vis detector set at 280 nm. The main peptide or PEG−peptide conjugate peak was integrated and analyzed relative to the peak area at t = 0 and its disappearance monitored over approximately 100 min. The relative peak area (A_t/A_0) was fitted with a first-order exponential decay

$$A_t = A_0 \exp(-kt) \quad (3)$$

where A_t is the area at a specific time, t, A_0 is the peak area at t = 0, and k is the rate constant from which the degradation half-life, $t_{1/2}$ can be defined as

$$t_{1/2} = \ln 2/k \quad (4)$$

Syncytia Assay. Twenty-four hours prior to commencing the assay, CHO-WT cells expressing the HIV-1 IIIB gp120 and gp41 proteins were seeded in GMEM and 10% FCS in 6-well plates with 2.5 × 10^5 cells at 2 mL/well.

On the day of the assay, approximately 6 × 10^5 SupT1 cells (or CD4-negative K652 cells as a negative control) were counted with a Neubauer chamber followed by 5 min centrifugation at 1500 rpm. The supernatant was removed and the cells were washed with approximately 5 mL RPMI medium and centrifuged once more at 1500 rpm for 5 min. After removal of the supernatant, the cells were washed in serum free RPMI and then incubated with 5 μM CTOrange dye, suspended in serum free RPMI medium, for 20 min at 37 °C. The cells were centrifuged at 1500 rpm and washed three times with 5 mL mixture of RPMI medium and 10% FCS followed by resuspension of the SupT1 (or K652) cells in 6 mL RPMI medium with 10% FCS. The wells containing CHO-WT cells were washed with 2 mL serum free GMEM followed by the addition of 2 mL CellTracker Green (5 μM, CTgreen) dye suspended in GMEM-SF medium and 20 min incubation at 37 °C. The cells were washed twice with 2 mL GMEM + 10% FCS after which 1 mL of peptide or PEG−peptide conjugate dissolved at a 2-fold higher concentration than desired for the assay was added to the wells with CHO-WT. The concentrations of the peptide and PEG−peptide conjugates in the solutions that were added to the well containing CHO-WT cells were determined by UV−vis spectrophotometry at 280 nm using the extinction coefficient determined from the linear combination of the molar extinction coefficients from tyrosine and tryptophan.[27]

To assess the membrane fusion inhibitory efficacy of the peptide and peptide conjugates, 1 mL (1 × 10^5 cells) CTOrange stained SupT1 (or K652) cells were added to the wells containing the CTgreen stained CHO-WT cells and the peptide or peptide−conjugate and subsequently incubated for 4 h at 37 °C. The nonadherent cells were removed and the wells were washed twice with 2 mL HBSS. Finally, the cells were fixed using ice-cold 70% methanol (kept at −20 °C) and incubated at 4 °C for 15 min. Subsequently, the methanol was removed and the wells were washed with HBSS medium. As a negative control, exactly the same protocol was followed for the preparation of the CD4 negative K652 cells. The K652 cells do not have the CD4 receptor and therefore do not fuse with CHO-WT cells to form syncytia. K652 cells were used as a control to prove that the formation of syncytia was due to fusion of membranes as a result of the CHO-WT envelope protein interaction with CD4 and not via another (unknown) mechanism.

The wells were analyzed using fluorescence microscopy monitoring the green channel and red channel. Cells were counted similarly as described by Muñoz-Barroso et al.[32] Briefly, fusion was quantified by counting the numbers of red

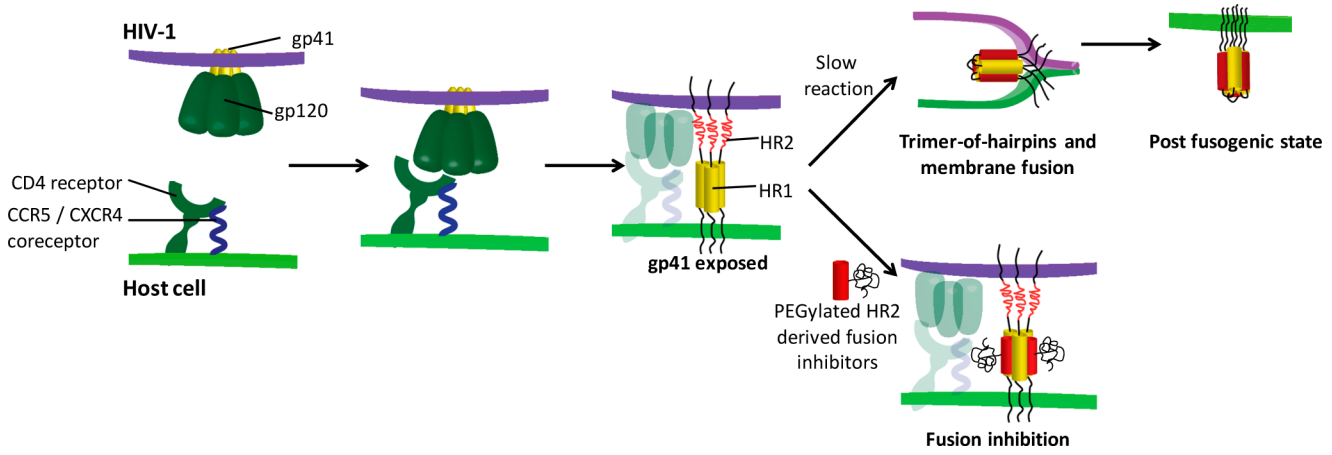

Figure 1. Schematic overview of the HIV-1–host cell membrane fusion process and its proposed inhibition by PEGylated HR2 derived fusion inhibitors.

Table 1. Sequences of the Peptide and Peptide–PEG Conjugates

Sample	*f c f c f c f c f*
WT	EWDREINN YTSLIHSLIEESQNQQEKNEQELLELDKWASLW
N terminus	CEWDREINN YTSLIHSLIEESQNQQEKNEQELLELDKWASLW
R4C	EWD**C**EINN YTSLIHSLIEESQNQQEKNEQELLELDKWASLW
S11C	EWDREINN YT**C**LIHSLIEESQNQQEKNEQELLELDKWASLW
S15C	EWDREINN YTSLIH**C**LIEESQNQQEKNEQELLELDKWASLW
E18C	EWDREINN YTSLIHSLI**C**ESQNQQEKNEQELLELDKWASLW
N22C	EWDREINN YTSLIHSLIEESQ**C**QQEKNEQELLELDKWASLW
Q29C	EWDREINN YTSLIHSLIEESQNQQEKNE**C**ELLELDKWASLW
C terminus	EWDREINN YTSLIHSLIEESQNQQEKNEQELLELDKWASLWC
S20C	EWDREINN YTSLIHSLIEE**C**QNQQEKNEQELLELDKWASLW

dx.doi.org/10.1021/bc3002248 | *Bioconjugate Chem.* 2012, 23, 1648–1660

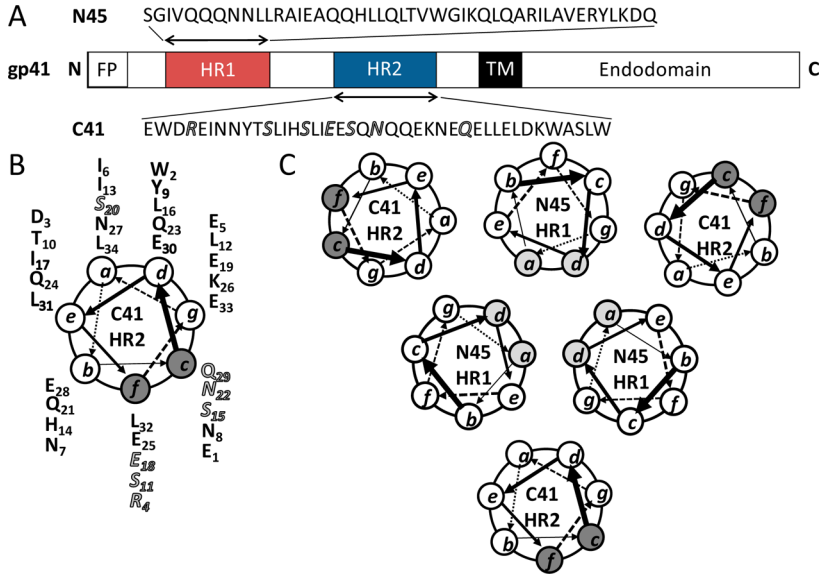

Figure 2. (A) Sequences of the HR1 derived peptide N45 and the HR2 derived peptide C41. (B) Helical wheel representation of the C41 peptide with residues mutated to cysteine highlighted in the *c* and *f* positions. (C) Helical wheel representation of the six-helix bundle formed by assembly of the 3 N45 and 3 C41 peptides. The sequences of the HR1 and HR2 domains are defined as published in ref 39, while the HR1 derived peptide sequence N45 is defined as published in ref 31.

(SupT1 derived) nuclei inside the syncytia relative to the number of nuclei inside the syncytia observed in the absence of peptide fusion inhibitor. Counting was facilitated using the cell counter plugin in *ImageJ* software.[33] This process was repeated for all peptide–PEG conjugates at concentrations between 0 and approximately 400 nM. The relative data were fitted with the following equation:

$$y = 1/(1 + [\text{peptide}]/\text{IC}_{50}) \quad (3)$$

where y is the normalized number of syncytia as a function of peptide concentration to deduce a concentration at which 50% of the syncytia are inhibited, IC_{50}. The standard error bars indicate variance of syncytia formation between three or more areas under the microscope from two independent assays.

RESULTS AND DISCUSSION

Conjugate Design and Synthesis. Fusion of the HIV-1 virus with a host cell proceeds via the formation of a six-helix bundle that has been identified as a trimer of antiparallel coiled-coil hairpins (Figure 1).[34,35] Formation of the fusion active trimer of hairpins starts with binding of the HIV-1 gp120 envelope glycoprotein, which is presented as trimers on the viral envelope, to a CD4 receptor and a CXCR4 or CCR5 coreceptor on the target cell.[34] This binding process induces a conformational change in gp120 and exposes gp41. Each gp41 protein contains two domains, HR1 and HR2, that each have the characteristic primary structural features of coiled coil forming peptides.[36] Successful HIV-1–host cell fusion involves intramolecular antiparallel heterodimerization of the HR1 and HR2 regions of all three gp41 glycoproteins that are present on the viral envelope.[35] Peptides derived from the HR1 and HR2 region have been successfully explored as competitive inhibitors to prevent the formation of the fusion active trimer of hairpins.[3,37,38]

To explore the PEGylation of these fusion inhibitors and, more specifically, study the effects of PEG molecular weight and site of conjugation on fusion inhibiting activity and proteolytic stability, a library of PEG–peptide conjugates based on the HR2 region of gp41 has been prepared (Table 1). To illustrate the rationale behind the synthesis of the PEGylated peptides listed in Table 1, Figure 2 presents the amino acid sequence of the HR2 region as well as helical wheel representations of a peptide derived from HR2 (C41, WT), both as a single helix and as part of the fusogenic six-helix bundle complex with the N45 peptide[31] derived from the HR1 region. The HR1 and HR2 regions are defined according to the heptad repeats as shown by Weissenhorn et al.[39] The design of the HR2 derived peptide C41 was based on the sequence of T-20[3] but with an extension at the N-terminal end to include the deep-pocket binding residues Trp-2 and Ile-6 that have been shown to increase antiviral potency,[40] while truncating the C-terminus of T-20, which is outside the heptad repeat region.[39] In addition to the N- and C-terminal amino acids of C41, residues 4, 11, 15, 18, 22, and 29, which are located at the *c* or *f* heptad position of the peptide, were targeted for PEGylation so as to minimize interference of the PEG chain with the formation of the six-helix bundle structure. To enable site-selective PEGylation, the appropriate residues in the wild-type HR2 sequence were replaced by cysteine. Selective N- and C-terminal PEGylation was achieved by extending the HR2 sequence with an additional cysteine residue at the desired chain end of the peptide. The sample names in Table 1 reflect these mutations and indicate the original amino acid in the HR2 sequence that was targeted, the position of this amino acid in the wild-type HR2 peptide, as well as the amino acid by which the wild-type residue was replaced (cysteine C in all cases). As negative controls, two conjugates (S20C) were prepared in which two different molecular weight PEGs were attached to the heptad position *a* of the HR2 peptide.

The PEGylated HR2 derivatives listed in Table 1 were prepared via a Michael-type addition reaction between an acrylate-modified monomethoxy poly(ethylene glycol) and the cysteine thiol group on the peptide (Supporting Information Scheme S1). The conjugates were purified and isolated by preparative HPLC and obtained in 60–90% yield. The PEG–peptide conjugates were characterized by MALDI-ToF mass

dx.doi.org/10.1021/bc3002248 | *Bioconjugate Chem.* 2012, 23, 1648–1660

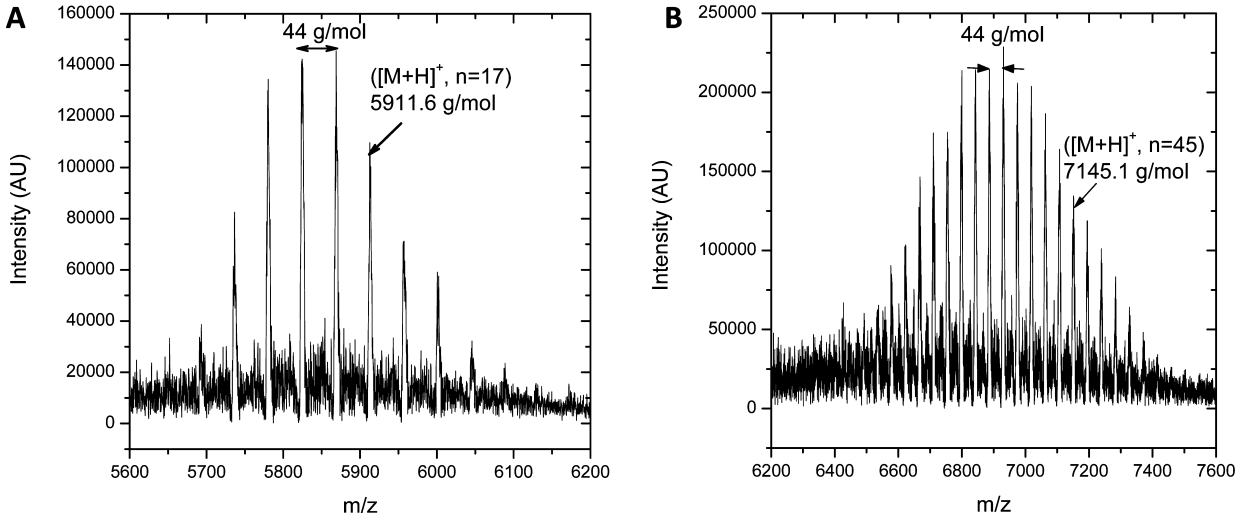

Figure 3. MALDI-ToF mass spectra of (A) the S15C-PEG750 and (B) the S15C-PEG2000 conjugates.

Table 2. Biophysical Characterization, Trypsin Degradation Half-Life ($t_{1/2}$), and Cell−Cell Fusion Inhibition Efficacy (IC_{50}) of the Peptides and Peptide−PEG Conjugates Investigated in This Study[a]

sample	MRE $-[\theta]_{222}$ (deg cm^2 dmol^{-1})	α-helical content (%)	N45:Sample $-[\theta]_{222}$ (deg cm^2 dmol^{-1})	N45:Sample α-helical content (%)	$t_{1/2}$ (min)	$t_{1/2}/t_{1/2,WT}$ (−)	IC_{50} (nM)
Wild type, WT	7700	22	28100	79	37.2	n. a.	1.5 ± 0.1
N-terminus	7100	20	17300	48	38.6	1.0	n.d.
N-terminus-PEG750	9300	26	23200	65	40.0	1.1	7.2 ± 0.7
N-terminus-PEG2000	9300	26	27500	77	79.3	2.1	11.2 ± 1.9
R4C	7000	20	23600	66	37.4	1.0	n.d.
R4C-PEG750	7900	22	24000	67	44.1	1.2	5.1 ± 1.1
R4C-PEG2000	8400	24	25800	72	67.4	1.8	8.7 ± 1.3
S11C	7800	22	18600	52	38.9	1.0	n.d.
S11C-PEG750	8100	23	22300	63	50.2	1.3	4.4 ± 0.8
S11C-PEG2000	7900	22	24700	69	91.0	2.4	4.9 ± 0.5
S15C	7400	21	16700	47	39.9	1.1	n.d.
S15C-PEG750	7700	22	22700	64	53.7	1.4	4.1 ± 1.0
S15C-PEG2000	8400	24	26100	73	82.4	2.2	5.0 ± 0.5
E18C	7700	22	18700	53	38.4	1.0	n.d.
E18C-PEG750	8100	23	23100	65	50.3	1.4	4.5 ± 1.0
E18C-PEG2000	7900	22	28300	79	81.3	2.2	4.9 ± 0.6
N22C	7900	22	22200	62	38.9	1.0	n.d.
N22C-PEG750	9400	26	22400	63	51.8	1.4	4.2 ± 0.9
N22C-PEG2000	8000	23	29100	82	80.7	2.2	5.1 ± 0.5
Q29C	7800	22	19700	55	38.6	1.0	n.d.
Q29C-PEG750	8200	23	21100	59	58.1	1.6	5.2 ± 0.8
Q29C-PEG2000	7000	20	27000	76	84.1	2.3	5.5 ± 0.5
C-terminus	7000	20	20700	58	39.0	1.0	n.d.
C-terminus-PEG750	9300	26	22500	63	81.2	2.2	10.9 ± 2.2
C-terminus-PEG2000	8700	25	23400	66	126.0	3.4	43.3 ± 14.8
S20C	7100	20	22000	62	38.6	1.0	n.d.
S20C-PEG750	8600	24	16300	46	42.0	1.1	>400
S20C-PEG2000	9500	27	16700	47	76.3	2.1	>400

[a]n.d. = not determined.

spectrometry. As a typical example, the MALDI-ToF mass spectra of S15C-PEG750 and S15C-PEG2000 are shown in Figure 3. The MALDI-ToF mass spectra for all other conjugates listed in Table 1 are included in the Supporting Information Figures S3 and S4. The mass spectra are characterized by a series of peaks that are spaced 44 Da apart, which corresponds to the mass of a single ethylene glycol repeat unit and reflects the chain length heterogeneity of the PEG chain. In Figure 3A,B, a representative peak is labeled with its respective mass that corresponds to the sum of the mass of the peptide and the mass of an integer number of ethylene glycol units (17 for PEG750 and 45 for PEG2000 in the spectra in Figure 3).

dx.doi.org/10.1021/bc3002248 | Bioconjugate Chem. 2012, 23, 1648−1660

Biophysical Characterization. The putative mode of action of the PEG−peptide conjugates listed in Table 1 involves binding to the complementary HR1 domain of the virus bound gp41 glycoprotein to form a six helix bundle (see Figure 1). To obtain first insight into the potential of the PEG−peptide conjugates to inhibit the formation of a fusogenic trimer of hairpins, the secondary structure and assembly behavior of the PEGylated peptides were studied with circular dichroism spectroscopy (CD) and analytical ultracentrifugation sedimentation equilibrium experiments. In these experiments, the N45 peptide was used to mimic the HR1 domain of the gp41 viral envelope protein (Figure 2).[31]

The results of the CD experiments are summarized in Table 2 and Figure 4. The CD spectra in Figure 4A and the mean molar residue ellipticities and helical contents listed in Table 2 indicate that neither the replacement of the selected residues in the wild-type C41 peptide by cysteine nor the PEGylation strongly affects the largely unordered secondary structure. In several cases for the PEGylated HR2 peptides, helical contents of 22−26% were determined, which are slightly increased as compared to the respective non-PEGylated peptide.

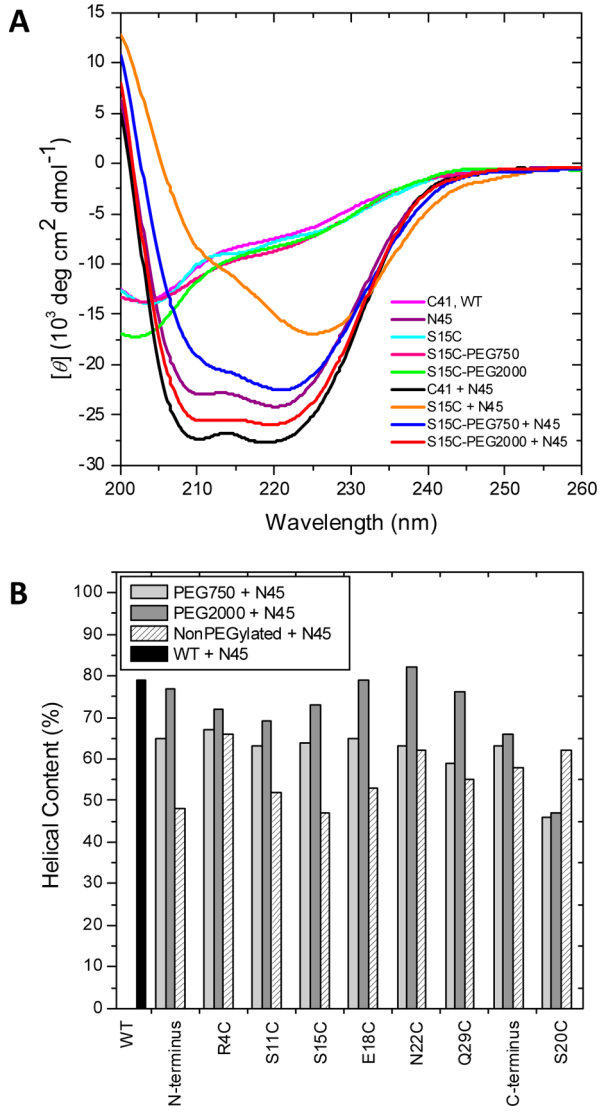

Figure 4. (A) CD spectra of the S15C non-PEGylated and PEG−peptide conjugates alone and in an equimolar mixture with N45. (B) Comparison of the helical contents of equimolar mixtures of wild-type, non-PEGylated peptides and PEG−peptide conjugates with N45.

Equimolar mixtures of the cysteine modified HR2 peptides and the N45 peptide afforded CD spectra that were indicative of α-helical structures but with $[\theta_{222}]/[\theta_{208}]$ values equal to ~0.78, which is lower than expected for a coiled coil. The α-helical contents that were determined for stoichiometric mixtures of the cysteine modified HR2 derivatives and N45 were lower than that of a stoichiometric mixture of the wild-type HR2 peptide (C41) and N45 indicating that the cysteine residue distorts the formation of the coiled coil superstructures. It is interesting to note that the S20C peptide, which contains a cysteine residue at an unfavorable *a* position of the heptad repeat, does not behave much differently from the other peptides which contain cysteine residues at positions that are anticipated to interfere less with coiled coil formation.

The PEGylated HR2 derivatives when mixed with an equimolar quantity of N45 produced CD spectra that are characteristic of coiled coil assemblies with relatively high α-helix contents (59−82%) and $[\theta_{222}]/[\theta_{208}]$ values of ~1. With the exception of the S20C derivatives, all of the investigated PEG−peptide samples showed higher α-helical contents in the presence of an equimolar amount of the N45 peptide as compared to a stoichiometric mixture of the corresponding non-PEGylated peptide and N45, which points toward a stabilizing effect of the PEG chain on the coiled coil assemblies. In all cases, the helical contents of the PEG2000 conjugates were higher than that of the PEG750 conjugates. The relatively low helical contents of the PEGylated S20C derivatives are in agreement with the conjugation site of this peptide and indicate that, as expected, PEGylation at the *a* position of the heptad repeat hampers "coiled coil" formation (*vide infra*).

To further assess the ability of the PEGylated peptides to form a six-helix bundle-type assembly in the presence of a stoichiometric amount of the HR1-derived N45 peptide, analytical ultracentrifugation experiments were carried out. As a typical example, Figure 5 shows the results of sedimentation equilibrium experiments that were performed on equimolar mixtures of the PEGylated S15C peptides and N45. Fitting of the data afforded molar masses of 32.8 kDa and 37.4 kDa for the PEG750 and PEG2000 based assemblies, which are within 3% of the expected masses of the corresponding six-helix bundles (33.4 kDa and 36.3 kDa for S15C-PEG750 and S15C-PEG2000, respectively). Sedimentation equilibrium experiments with the N- and C-terminally PEGylated HR2 peptide afforded molar masses of 32.3 kDa and 36.1 kDa for N-terminal-PEG750 and N-terminal-PEG2000 conjugates, respectively, and similarly 32.0 kDa and 35.9 kDa for C-terminal-PEG750 and C-terminal-PEG2000 conjugates, respectively. These molar masses agree well with expected molar masses of 33.7 kDa and 37.3 kDa for the C-/N-terminal-PEG750 and C-/N-terminal-PEG2000 conjugates, respectively (see Figure S5). Analytical ultracentrifugation studies of the S20C-PEG conjugates with N45 did not yield any sedimentation equilibrium curves, suggesting that the former did not form six-helix bundle structures. Taken together, the results from the CD and analytical ultracentrifugation experiments indicate that, with judicious control of the site of conjugation, PEGylation does not impair the self-assembly properties of the peptides.

Fusion Inhibition. To assess their membrane fusion inhibitory efficacy, the PEGylated HR2 peptides were investigated in a model cell−cell-based fusion assay, which involved an adherent Chinese Hamster Ovarian cell line

dx.doi.org/10.1021/bc3002248 | *Bioconjugate Chem.* 2012, 23, 1648−1660

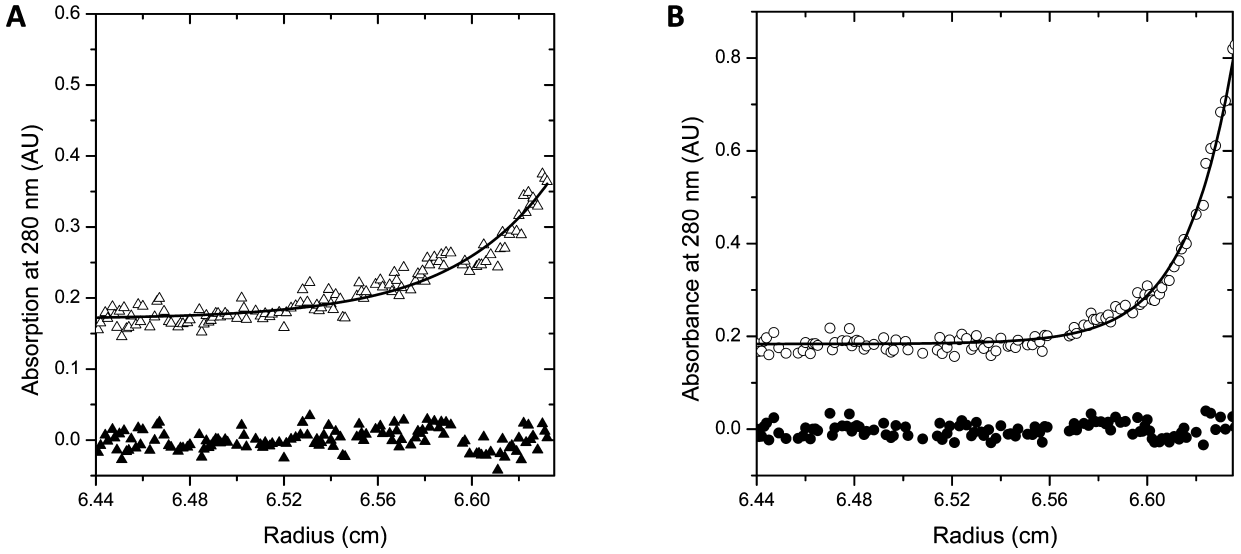

Figure 5. Results of sedimentation equilibrium experiments on equimolar mixtures of 10 μM N45 and 10 μM (A) S15C-PEG750 or (B) S15C-PEG2000 conjugates performed at 25 000 rpm over 24 h. The open symbols are the data points obtained from the sedimentation equilibrium experiment and the filled symbols are the residuals.

expressing the HIV-1 gp120 and gp41 surface proteins (CHO-WT)[25] and the CD4 positive SupT1[41] cell line. In the absence of a fusion inhibitor, addition of SupT1 cells to wells containing CHO-WT cells results in fusion of the cells, of which multiple fusion events lead to large cell-like structures with multiple nuclei known as syncytia.[25] To measure the fusion inhibitory efficacy of the PEGylated HR2 peptides, aliquots of the conjugates at concentrations ranging from 0 to 500 nM were added to a mixture of the CHO-WT and SupT1 cells and the number of syncytia counted after 4 h (SI Figure S6). From these experiments, dose–response curves, which represent the relative number of syncytia as a function of the concentration of the PEG–peptide conjugate, were obtained. As a representative example, the dose–response curves for three different conjugates are shown in Figure 6. Data for all the other conjugates are included in the Supporting Information (Figure S7). For each conjugate, the dose–response curve affords an IC_{50} value, which is used as a measure for the fusion inhibitory efficacy of that particular compound and represents the concentration of the PEG–peptide conjugate at which 50% of the relative number of syncytia were inhibited. The IC_{50} values for all PEG–peptide conjugates are included in Table 2 and also summarized in Figure 7.

With the exception of the S20C conjugates, the IC_{50} values determined for the PEGylated HR2 peptides varied between 4 and 40 nM. For the S20C-PEG750 and S20C-PEG2000 conjugates, IC_{50} values >400 nM were found. This is consistent with the low helical contents measured by CD and the lack of evidence of the formation of a six-helix bundle by analytical ultracentrifugation for these samples in the presence of an equimolar amount of the N45 peptide (*vide supra*). The results obtained with the S20C conjugates reflect the steric blocking of the unfavorably positioned PEG chains that prevent association of the HR2-derived peptide conjugates with the complementary HR1 domain of the gp41 protein on the CHO-WT cell surface. The data in Table 2 and Figure 7 indicate that PEGylation results in a decrease in the fusion inhibitory efficacy as compared to the wild-type peptide, but also demonstrate that the reduction in efficacy very much depends on the site of PEGylation. PEGylation at or near the N- or C-terminus is most unfavorable as evidenced from the IC_{50} values of the N-terminus, R4C, and C-terminus modified peptides. The IC_{50} values of the C-terminal-PEG750 and C-terminal-PEG2000 samples are significantly higher than those of the corresponding N-terminal PEGylated peptides. This may be related to the antiparallel orientation of the HR2 and HR1 peptides in the six-helix bundle structure,[42] which places the C-terminus of the HR2 peptide in closer proximity to the host cell membrane and makes the formation of this assembly, and thus fusion inhibition, more susceptible to the introduction of sterically demanding groups such as the PEG chains. These results also follow a similar trend obtained by Stoddart et al. with human serum albumin–C34 peptide conjugates, where conjugation of human serum albumin to the C-terminus of the C34 peptide resulted in an order-of-magnitude loss in efficacy relative to the unconjugated peptide and N-terminal conjugation.[23] Variation of the site of PEGylation from position 11, 15, 18, 22, or 29 in the HR2 sequence, in contrast, was not found to result in statistically significant variations in the IC_{50} values, irrespective of the PEG molecular weight. PEGylation at these positions resulted in IC_{50} values around 4.5 nM, which represents a 3-fold reduction in efficacy as compared to the wild-type, unmodified peptide. The only relatively moderate reduction in efficacy (in comparison to the N- and C-terminal PEGylated analogues) indicates that side chain as opposed to peptide chain end PEGylation imposes fewer steric constraints on the formation of the putative six-helix bundle structure and, as a consequence, fusion inhibition. The results of the fusion inhibition experiments emphasize that judicious choice of the site of PEGylation allows one to minimize detrimental steric effects that may impair the therapeutic efficacy of the PEG–peptide conjugates. Furthermore, slight losses in therapeutic efficacy may be compensated for by the increase in half-life of the HR2 peptides as has been observed with other PEGylated peptides and proteins (*vide infra*).[12,17,18,43]

Enzymatic Degradation. Since one of the major limitations of peptide/protein based drugs is their susceptibility to enzymatic degradation, a final series of model experiments was performed to study the influence of PEGylation on the degradation of the PEG–peptide conjugates. These experi-

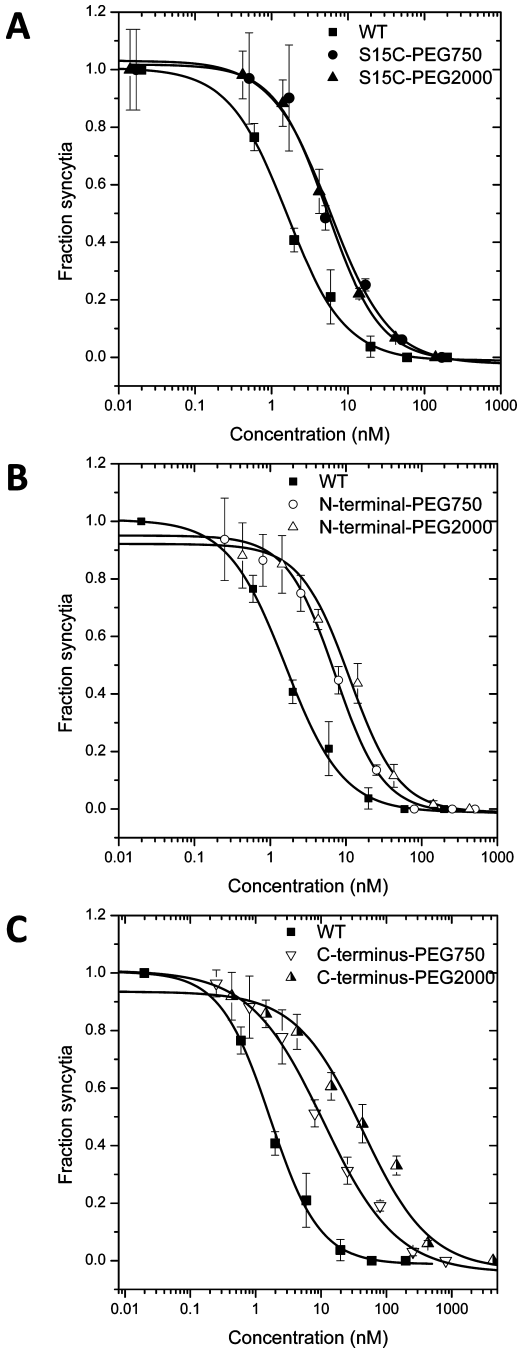

Figure 6. Dose–response curves obtained from the cell–cell fusion assay with (A) the S15C PEGylated, (B) the N-terminal PEGylated, and (C) the C-terminal PEGylated HR2 derived peptides. In each of the graphs, the dose–response curve of the wild-type HR2 derived peptide is included for comparison. If the error bars are not visible, they fall into the data point.

ments were carried out using the serine protease trypsin as a model enzyme. Trypsin was selected, as it is cheap and readily available and selectively cleaves amide bonds at the C-terminal side of positively charged lysine and arginine,[44] which facilitates the analysis of degradation products by analytical HPLC. Degradation experiments were performed over a time frame of approximately 100 min by incubating a 10 μM solution of the peptide or PEG–peptide conjugate with 1 μM trypsin. At regular time intervals, aliquots were taken and added to a solution containing the trypsin inhibitor phenylmethanesulfonyl fluoride in order to stop the degradation process. The aliquots were subsequently analyzed by reverse-phase HPLC. As a representative example, Figure 8A shows a series of HPLC chromatograms that were recorded on samples taken during the degradation of the wild-type peptide, C41. The chromatogram at t = 2 min shows a single peak (retention time = 14.2 min) corresponding to the intact wild-type peptide. With increasing incubation time, a second peak at a retention time of 13.1 min appears. Using electrospray ionization mass spectrometry, this peak was identified as being due to the N-terminal fragment WASLW-NH_2 (Figure 8B). The area of the main peak was determined via integration and plotted against time. As an example, Figure 8C shows the degradation profile of the wild-type peptide, as well as the S15C-PEG750 and S15C-PEG2000 conjugates. The resulting degradation curves were fitted with a single exponential decay, from which the trypsin degradation half-lives of the non-PEGylated and PEGylated peptides were determined. The degradation half-lives ($t_{1/2}$) of the wild-type peptide, the cysteine modified variants, and the PEG–peptide conjugates are summarized in Table 2 and Figure 9. The data illustrate that PEGylation is an effective strategy to increase the degradation half-life of the peptides. Whereas conjugation of a short PEG chain only leads to moderate improvements, the introduction of a longer PEG chain (PEG2000) increases the trypsin degradation half-life by a factor of 1.8–3.4. Analysis of the degradation half-lives as a function of the site of PEGylation in most cases only reveals minor variations and no real trends. The degradation half-lives of the PEG750 conjugates seem to gradually increase as the site of PEGylation shifts progressively closer to the C-terminus of the peptide, which may be due to the fact that trypsin cleaves at the C-terminal site of the targeted amide bond. The degradation half-lives of the C-terminus PEG750 and C-terminus PEG2000 conjugates, however, clearly stand out, for reasons which are unclear at the moment.

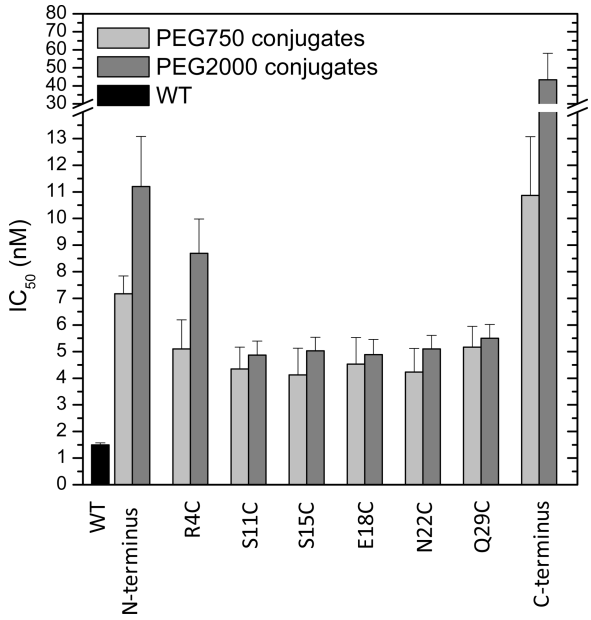

Figure 7. Comparison of the fusion inhibition efficacies of the PEG750 and PEG2000 peptide conjugates.

dx.doi.org/10.1021/bc3002248 | *Bioconjugate Chem.* 2012, 23, 1648–1660

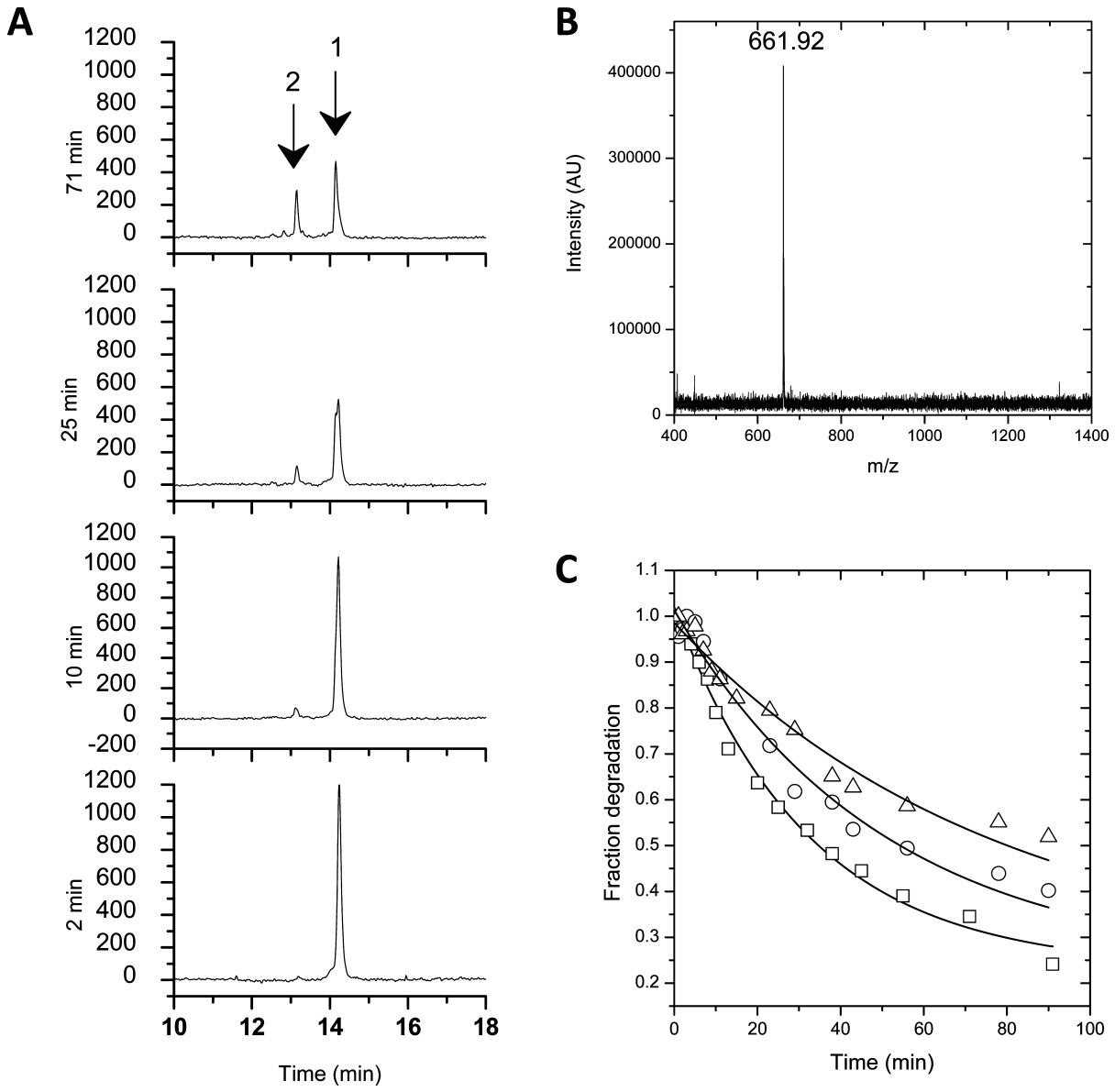

Figure 8. Enzymatic degradation of the wild-type peptide and the PEG-peptide conjugates. (A) Typical analytical reverse-phase HPLC chromatograms of wild-type peptide digests at 2, 10, 25, and 71 min. Peak 1 (retention time = 14.2 min) is the main peak that corresponds to the intact peptide and peak 2 (retention time = 13.1 min) refers to the fragment WASLW-NH_2. (B) The ESI mass spectrum of the isolated fragment peak 2. (C) Comparison of main peak areas as a function of time for the wild-type peptide (squares), S15C-PEG750 (circles), and S15C-PEG2000 conjugates (triangles).

■ CONCLUSIONS

This contribution has investigated the PEGylation of HIV-1 fusion inhibitors derived from the HR2 domain of the HIV-1 gp41 envelope glycoprotein. The specific aim of this study was to systematically investigate the influence of the site of PEGylation and PEG molecular weight on the biological activity and proteolytic stability of these peptides. The results of this study demonstrate that judicious choice of the site of conjugation enables access to PEGylated HR2 derivatives with only slightly reduced fusion inhibitory efficacies as compared to the non-PEGylated peptide, but with significantly improved proteolytic stabilities. PEGylation at positions *c* and *f* of the heptad repeat of the HR2 peptide places the PEG chain at the noninteracting surface of this peptide in its helical conformation. CD and analytical ultracentrifugation experiments demonstrated that these PEG-peptides form a six-helix bundle structure in the presence of an equimolar amount of a complementary HR1-derived peptide. Introducing the PEG chain at position *a* of the heptad repeat, which is located at the interacting interface of the helix, however, prevented the formation of the six-helix bundle structure. The fusion inhibition efficacy of the PEG−peptide conjugates was assessed in model cell−cell fusion experiments. Whereas conjugation of PEG2000 at the N- and C-terminus of the peptide resulted in a 7.5- and 29-fold reduction in fusion inhibitory efficacy, respectively, modification along the non-interacting helical surface of the peptide led only to a 3.3−5.8-fold reduction of efficacy as compared to the wild-type peptide. Similarly, conjugation of PEG750 to the N- and C-terminus resulted in a 4.8- and 7.3-fold reduction in efficacy, respectively, whereas side chain PEGylation only led to a 2.7−3.4-fold decrease in the fusion inhibitory efficacy. At the same time, however,

dx.doi.org/10.1021/bc3002248 | *Bioconjugate Chem.* 2012, 23, 1648−1660

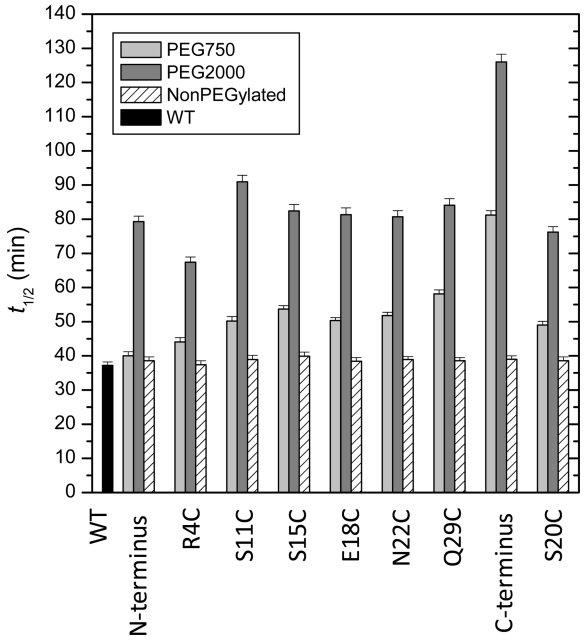

Figure 9. Comparison of the trypsin degradation half-lives of the wild-type peptide, the cysteine-modified variants, and the PEG−peptide conjugates. The error bars represent the error from the nonlinear fitting procedure.

modification of the peptides with PEG2000 led to a 1.8−3.4-fold increase in the trypsin degradation half-life. The results of this study emphasize the potential of site-specific PEGylation to modify therapeutic peptides and proteins and improve their stability, while minimizing adverse effects on bioactivity.

■ ASSOCIATED CONTENT

Supporting Information

Additional ^{1}H NMR and MALDI-ToF mass spectra of the PEG-acrylates and PEG-peptide conjugates, as well as analytical ultracentrifugation and cell−cell fusion inhibition micrographs and data. This material is available free of charge via the Internet at http://pubs.acs.org.

■ AUTHOR INFORMATION

Corresponding Author

*E-mail Address: Harm-Anton.Klok@epfl.ch.

Notes

The authors declare no competing financial interest.

■ ACKNOWLEDGMENTS

This work was supported by the European Commission, FP6 project 'NanoBioPharmaceutics' (NMP4-CT-2006-026723).

■ REFERENCES

(1) Cohen, J. (2007) New estimates scale back scope of HIV/AIDS epidemic. *Science 318*, 1360−1361.

(2) Mehellou, Y., and De Clercq, E. (2010) Twenty-six years of anti-HIV drug discovery: Where do we stand and where do we go? *J. Med. Chem. 53*, 521−538.

(3) Wild, C., Greenwell, T., and Matthews, T. (1993) A synthetic peptide from HIV-1 gp41 is a potent inhibitor of virus-mediated cell-cell fusion. *AIDS Res. Hum. Retroviruses 9*, 1051−1053.

(4) De Clercq, E. (2009) Anti-HIV drugs: 25 compounds approved within 25 years after the discovery of HIV. *Int. J. Antimicrob. Agents 33*, 307−320.

(5) Eggink, D., Berkhout, B., and Sanders, R. W. (2010) Inhibition of HIV-1 by fusion inhibitors. *Curr. Pharm. Des. 16*, 3716−3728.

(6) Fuzeon Product Information, http://www.fuzeon.com.

(7) Veronese, F. M. (2001) Peptide and protein PEGylation: A review of problems and solutions. *Biomaterials 22*, 405−417.

(8) Caliceti, P., and Veronese, F. M. (2003) Pharmacokinetic and biodistribution properties of poly(ethylene glycol)-protein conjugates. *Adv. Drug Delivery Rev. 55*, 1261−1277.

(9) Pasut, G., and Veronese, F. M. (2007) Polymer-drug conjugation, recent achievements and general strategies. *Prog. Polym. Sci. (Oxford, U.K.) 32*, 933−961.

(10) Klok, H.-A. (2009) Peptide/protein - synthetic polymer conjugates - Quo vadis. *Macromolecules 42*, 7990−8000.

(11) Caliceti, P., Salmaso, S., Walker, G., and Bernkop-Schnurch, A. (2004) Development and in vivo evaluation of an oral insulin-PEG delivery system. *Eur. J. Pharm. Sci. 22*, 315−323.

(12) Bailon, P., Palleroni, A., Schaffer, C. A., Spence, C. L., Fung, W. J., Porter, J. E., Ehrlich, G. K., Pan, W., Xu, Z. X., Modi, M. W., Farid, A., and Berthold, W. (2001) Rational design of a potent, long-lasting form of interferon: A 40 kDa branched polyethylene glycol-conjugated interferon α-2a for the treatment of hepatitis C. *Bioconjugate Chem. 12*, 195−202.

(13) Kochendoerfer, G. G., Chen, S. Y., Mao, F., Cressman, S., Traviglia, S., Shao, H., Hunter, C. L., Low, D. W., Cagle, E. N., Carnevali, M., Gueriguian, V., Keogh, P. J., Porter, H., Stratton, S. M., Con Wiedeke, M., Wilken, J., Tang, J., Levy, J. J., Miranda, L. P., Crnogorac, M. M., Kalbag, S., Botti, P., Schindler-Horvat, J., Savatski, L., Adamson, J. W., Kung, A., Kent, S. B. H., and Bradburne, J. A. (2003) Design and chemical synthesis of a homogeneous polymer-modified erythropoiesis protein. *Science 299*, 884−887.

(14) Roberts, M. J., Bentley, M. D., and Harris, J. M. (2002) Chemistry for peptide and protein PEGylation. *Adv. Drug Delivery Rev. 54*, 459−476.

(15) Gauthier, M. A., and Klok, H.-A. (2008) Peptide/protein-polymer conjugates: Synthetic strategies and design concepts. *Chem. Commun.*, 2591−2611.

(16) Bailon, P., and Won, C. Y. (2009) PEG-modified biopharmaceuticals. *Expert Opin. Drug Delivery 6*, 1−16.

(17) Doherty, D. H., Rosendahl, M. S., Smith, D. J., Hughes, J. M., Chlipala, E. A., and Cox, G. N. (2005) Site-specific PEGylation of engineered cysteine analogues of recombinant human granulocyte-macrophage colony-stimulating factor. *Bioconjugate Chem. 16*, 1291−1298.

(18) Salhanick, A. I., Clairmont, K. B., Buckholz, T. M., Pellegrino, C. M., Ha, S., and Lumb, K. J. (2005) Contribution of site-specific PEGylation to the dipeptidyl peptidase IV stability of glucose-dependent insulinotropic polypeptide. *Bioorg. Med. Chem. Lett. 15*, 4114−4117.

(19) Yamamoto, Y., Tsutsumi, Y., Yoshioka, Y., Nishibata, T., Kobayashi, K., Okamoto, T., Mukai, Y., Shimizu, T., Nakagawa, S., Nagata, S., and Mayumi, T. (2003) Site-specific pegylation of a lysine-deficient TNF-α with full bioactivity. *Nat. Biotechnol. 21*, 546−552.

(20) Welch, B. D., VanDemark, A. P., Heroux, A., Hill, C. P., and Kay, M. S. (2007) Potent D-peptide inhibitors of HIV-1 entry. *Proc. Natl. Acad. Sci. U.S.A. 104*, 16828−16833.

(21) Bailon, P. S., and Won, C.-Y. (2004) PEGylated T20 Polypeptide. WO/2004/013164.

(22) Bailon, P. S., and Won, C.-Y. (2004) PEGylated T1249 Polypeptide. WO/2004/013165.

(23) Stoddart, C. A., Nault, G., Galkina, S. A., Thibaudeau, K., Bakis, P., Bousquet-Gagnon, N., Robitaille, M., Bellomo, M., Paradis, V., Liscourt, P., Lobach, A., Rivard, M. È., Ptak, R. G., Mankowski, M. K., Bridon, D., and Quraishi, O. (2008) Albumin-conjugated C34 peptide HIV-1 fusion inhibitor: Equipotent to C34 and T-20 in vitro with sustained activity in SCID-HU THY/LIV mice. *J. Biol. Chem. 283*, 34045−34052.

(24) Huet, T., Kerbarh, O., Schols, D., Clayette, P., Gauchet, C., Dubreucq, G., Vincent, L., Bompais, H., Mazinghien, R., Querolle, O., Salvador, A., Lemoine, J., Lucidi, B., Balzarini, J., and Petitou, M.

(2010) Long-lasting enfuvirtide carrier pentasaccharide conjugates with potent anti-human immunodeficiency virus type 1 activity. *Antimicrob. Agents Chemother. 54*, 134−142.
(25) Weiss, C. D., and White, J. M. (1993) Characterization of stable Chinese hamster ovary cells expressing wild- type, secreted, and glycosylphosphatidylinositol-anchored human immunodeficiency virus type 1 envelope glycoprotein. *J. Virol. 67*, 7060−7066.
(26) Palasek, S. A., Cox, Z. J., and Collins, J. M. (2007) Limiting racemization and aspartimide formation in microwave-enhanced Fmoc solid phase peptide synthesis. *J. Pept. Sci. 13*, 143−148.
(27) Pace, C. N., Vajdos, F., Fee, L., Grimsley, G., and Gray, T. (1995) How to measure and predict the molar absorption coefficient of a protein. *Protein Sci. 4*, 2411−2423.
(28) Chen, Y. H., Yang, J. T., and Chau, K. H. (1974) Determination of the helix and β form of proteins in aqueous solution by circular dichroism. *Biochemistry 13*, 3350−3359.
(29) http://www.jphilo.mailway.com/download.htm.
(30) http://www.analyticalultracentrifugation.com/sedphat/sedphat.htm.
(31) Dwyer, J. J., Hasan, A., Wilson, K. L., White, J. M., Matthews, T. J., and Delmedico, M. K. (2003) The hydrophobic pocket contributes to the structural stability of the N-terminal coiled coil of HIV gp41 but is not required for six-helix bundle formation. *Biochemistry 42*, 4945−4953.
(32) Muñoz-Barroso, I., Durell, S., Sakaguchi, K., Appella, E., and Blumenthal, R. (1998) Dilation of the human immunodeficiency virus-1 envelope glycoprotein fusion pore revealed by the inhibitory action of a synthetic peptide from gp41. *J. Cell Biol. 140*, 315−323.
(33) http://rsbweb.nih.gov/ij/.
(34) Gallo, S. A., Finnegan, C. M., Viard, M., Raviv, Y., Dimitrov, A., Rawat, S. S., Puri, A., Durell, S., and Blumenthal, R. (2003) The HIV Env-mediated fusion reaction. *Biochim. Biophys. Acta 1614*, 36−50.
(35) Chan, D. C., and Kim, P. S. (1998) HIV entry and its inhibition. *Cell 93*, 681−684.
(36) Lu, M., Blacklow, S. C., and Kim, P. S. (1995) A trimeric structural domain of the HIV-1 transmembrane glycoprotein. *Nat. Struct. Biol. 2*, 1075−1082.
(37) Bianchi, E., Finotto, M., Ingallinella, P., Hrin, R., Carella, A. V., Hou, X. S., Schleif, W. A., Miller, M. D., Geleziunas, R., and Pessi, A. (2005) Covalent stabilization of coiled coils of the HIV gp41 N region yields extremely potent and broad inhibitors of viral infection. *Proc. Natl. Acad. Sci. U.S.A. 102*, 12903−12908.
(38) Eggink, D., Langedijk, J. P. M., Bonvin, A. M. J. J., Deng, Y., Lu, M., Berkhout, B., and Sanders, R. W. (2009) Detailed mechanistic insights into HIV-1 sensitivity to three generations of fusion inhibitors. *J. Biol. Chem. 284*, 26941−26950.
(39) Weissenhorn, W., Dessen, A., Harrison, S. C., Skehel, J. J., and Wiley, D. C. (1997) Atomic structure of the ectodomain from HIV-1 gp41. *Nature 387*, 426−430.
(40) Chan, D. C., Chutkowski, C. T., and Kim, P. S. (1998) Evidence that a prominent cavity in the coiled coil of HIV type 1 gp41 is an attractive drug target. *Proc. Natl. Acad. Sci. U.S.A. 95*, 15613−15617.
(41) Smith, S. D., Morgan, R., and Link, M. P. (1986) Cytogenetic and immunophenotypic analysis of cell lines established from patients with T cell leukemia/lymphoma. *Blood 67*, 650−656.
(42) Buzon, V., Natrajan, G., Schibli, D., Campelo, F., Kozlov, M. M., and Weissenhorn, W. (2010) Crystal structure of HIV-1 gp41 including both fusion peptide and membrane proximal external regions. *PLoS Pathog. 6*, e1000880.
(43) Rosendahl, M. S., Doherty, D. H., Smith, D. J., Carlson, S. J., Chlipala, E. A., and Cox, G. N. (2005) A long-acting, highly potent interferon α-2 conjugate created using site-specific PEGylation. *Bioconjugate Chem. 16*, 200−207.
(44) http://www.sigmaaldrich.com/life-science/metabolomics/enzyme-explorer/analytical-enzymes/trypsin.html.